Heat Treatment Influence on the Wear Behaviour of Titanium-Molybdenum Biomedical Alloys

ALEXANDRU GHIBAN[1]*, ANA EVA JIMENEZ BALLESTA[2], NOELIA GONZALEZ MORALES[2], LIVIU DANIEL PIRVULESCU[3], BRANDUSA GHIBAN[1], TUDOR VIOREL TIGANESCU[4]

[1] University Politehnica Bucharest, 313 Spl. Independetei, 060042, Bucharest, Romania

[2] Universidad Politecnica de Cartagena, Spain

[3] Casa Auto Timisoara, 142 Calea Sagului, 300516, Timisoara, Romania

[4] Technical Military Academy of Bucharest, 39-49 G. Cosbuc Blvd., 050141, Bucharest, Romania

In present paper there are given the results concerning wear behaviour in Ringer's solution of four titanium alloys with 5%Mo, 7%Mo, 11%Mo and 12%Mo. Structural investigations (made by both optic, electronic microscopy and X-Rays diffraction) revealed a dual phase structure consisting from alpha martensite and beta"solid solution, with the constituents proportion depending on molybdenum content. Wear rates were determined using a Talysurf profilometer in Ringer's solution for the experimental titanium-molybdenum alloys. Finally, the beneficial influence of molybdenum on wear behavior was put in evidence: the higher molybdenum content is, the lower friction coefficient is.

Keywords: titanium alloying, wear, heat treatment, profilometer

Titanium and titanium alloys are widely used for many biomedical applications due to their low density, excellent biocompatibility, corrosion resistance and mechanical properties. Among the various types of Ti alloys, Ti-6Al-4V has been the choice in many situations [1, 2]. But the Young's modulus of elasticity of this alloy, (about 105-108 GPa) despite that being half of the CoCrMo alloys (210GPa), and 316L stainless steels (200GPa) [3], is still much larger than the Young's modulus of bone (10-30GPa), which leads to stress shielding, or even bone resoption around the implant [4]. Therefore, the mechanical properties of structural biomaterials in a living body environment – such as fatigue, toughness, and wear resistance – need to be evaluated and then improved in order to confidently use the implants for a long period of time. Many researchers are agree that freeting corrosion between bone cement and metallic femoral stem (implant) is one of the major factors of the loosening of total joint replacement, as is illustrated in figure 1 [5, 6].

Recent studies inform about the release of aluminum and vanadium used in Ti-6Al-4V alloy was found to be toxic and their accumulation in the surrounding tissue was of great concern [7, 30, 31]. Consequently, effort was diverted towards the development of Ti based biomaterials free from Al and V. Furthermore, it was noted that these α or $\alpha+\beta$ alloys have an elastic modulus significantly higher than the elastic modulus of implant and bone. In order to overcome this drawback, β Ti alloys were developed with the aid of β stabilising elements such as Nb, Mo, Zr and Ta. β Ti alloys were found to have enhanced biocompatibility and increased compatibility with the mechanical properties of bone and implants [8, 9]. It is noted [9-15] that the corrosion rate of two-phase Ti alloys is higher in physiological solution than single-phase Ti alloys. Thus β–Ti alloys have beneficial properties as potential materials for metallic stems in total joint replacement. In the present investigation, the wear behaviour was tested on different composition of newly β titanium alloys, along $\alpha+\beta$ alloy in Ringer's solution, in order to make the correlation between molybdenum content and wear behavior of β titanium alloys.

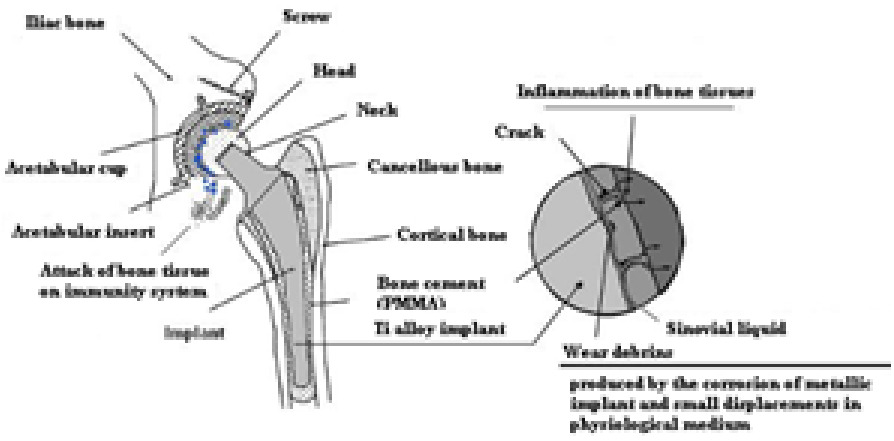

Fig.1. Scheme of wear mechanim in implat after [5, 6]

* email: alexandru.ghiban@gmail.com

Alloy	Chemical composition, wt. %						
	Mo	Al	C	Fe	Sn	Zr	V
$TiMo_5$	5.16	0.0067	0.015	0.033	0.85	0.021	0.0090
$TiMo_7$	6.98	0.023	0.016	0.050	1.09	0.0015	0.017
$TiMo_{11}$	10.98	0.025	0.016	0.038	1.48	0.0025	0.017
$TiMo_{12}$	11.94	0.0037	0.014	0.028	1.46	0.0030	0.011

Table 1
CHEMICAL COMPOSITION OF THE EXPERIMETAL ALLOYS FROM THE Ti-Mo SYSTEM

Experimental part

Materials and methods

The chemical composition of the experimental alloys produced by the method RAV was determined by spectral analysis using an optical spark emission spectrometer, as is given in table 1.

TiMo phase constitution of the experimental alloys was identified both by metallographic analysis and by X-ray diffraction. Investigations on optical microscope were carried out on a Reichert microscope equipped with Image Pro software. X-ray diffraction analysis was performed on a DRON 3 Kα copper radiation and scanning electron microscopy analysis was performed on a microscope Phylips equipped with specialized software. In order to define the best heat treatment applied on experimental TiMo alloys, heat treatments were made with air cooling, and respectively water. Annealing temperature was chosen less than beta solvus, respectively 950°C with keeping for one hour purposes of achieving the most stable β structure.

Wear behaviour of experimental TiMo alloys was performed with a Taylor Hobson Talysurf profilometer type CLI 500. It is an instrument for measuring surface topography. This involves measuring the height of a point at a given moment. Experimental samples were subjected to measurement of surface topography set on a sliding tray moving to explore complete measurement areas. Normally, the system is designed for contact-free measurement by using the optical lens with a single focal point of the sensor. By means of software associated with known Talymap, and the main points are measured topographical image generated by the Talysurf profilometer. Were measured at four points depth stained area in contact with the wear and later were calculated coefficient of friction and wear rate by using the following formula:

Slinding distance was calculated with the relation:

$$L = \frac{19.95nd}{\sqrt{\frac{d^2}{4} - 25}} \quad (1)$$

For solid materials, it is known the model for simple abrasion, based on Archard equation, with use for slinding distance the formula:

$$LF_N = \frac{V}{K} \quad \text{where b<<d, so:}$$

$$LF_N \approx \frac{1}{K}\left(\frac{\pi b^4}{32d}\right) \quad (2)$$

where L- slinding distance, F_N- normal applied force, V- volume of wear material, K- wear coefficient, b- diameter of wear print, d- diameter of sphere (respectively 25,4mm).

The value of the wear coefficient is determined with the relation:

$$\mu = \frac{\pi b^4}{32LF_N d} \quad (3)$$

The evaluation of the tribologic behaviour is made by:

- assessment of surface topography after testing at probilometer;

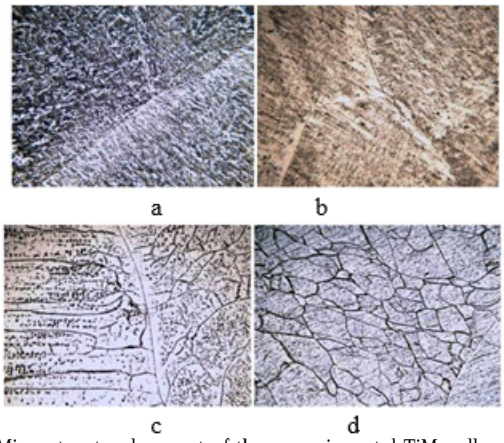

Fig. 2. Microstructural aspect of the experimental TiMo alloys: (a) alloy TiMo5 , (b) aloy TiMo7, (c) alloy TiMo11, (d) alloy TiMo12

- Maximum wear depth measurement and calculation of the wear material volume;

- determination of the friction coefficient, correlated with load test values;

- determining the wear rate.

Results and discussions

The microstructural aspects results of the experimental alloys by quantitative and qualitative optical metallographic analysis are shown in figure 2. Thus it can be seen one martensite phase and one phase of solid solution. Identification by X-ray diffraction (fig. 3) revealed the martensitic phase is orthorhombic α' martensite and the solid solution is b phase.

Metallographic analysis shows that alloys TiMo5 and TiMo7 have a dual structure, consisting of a high proportion of the orthorhombic martensite α' and a small amount of β solid solution. On increasing of molybdenum concentration, respectively on alloys TiMo11 and TiMo12, will be observed the quantitative of the β solid solution proportion increasing, and also a small quantity of completely orthogonal martensite.

The results are consistent with those obtained from the literature. In a recent study Ho [16], over a range of molybdenum concentrations in titanium alloys, observed the orthorhombic martensite over a content of 7.5% Mo. In a more recent study, Ho [17] revealed the structural changes induced by the presence of molybdenum, but in the alloy Ti-5Cr. Lin [18-20] investigated the system group alloys Ti-7,5Mo-Fe and obtained the presence of orthorhombic martensite phase along a small ω proportions, with a strengthener effect. Cheng [21] investigated four alloys from Ti-Mo system with other ratios of molybdenum than those in this paper, namely 5, 10, 15 and 20% and proposed the Ti-10Mo alloy for dental applications.

Oliveira [22] investigated the Ti-Mo system alloys with molybdenum in proportions of 4-20%, and observe the dominant phase b on the 10% Mo, with biomedical applications. Wu[23] made the structure correlations of the system alloys Ti-Mo-H (the proportion of molybdenum, up to 15%). Gordin[24, 25] studied the structural changes of two Ti-alloys, respectively Ti-8Mo and Ti-16Mo nitrided

at 1400° C which was highlighted of precipitated nitrides either in α or β solid solution. Gabriel [26] proposed a new alloy for biomedical applications, namely Ti-12Mo-3NB, with a b-phase structure. Zhou [27] studied the properties of two alloys, respectively Ti-10Mo and Ti-20Mo, but after plastic deformation and heat treatment, suggesting the alloy with 10% Mo for biomedical applications among other β Ti-Mo alloys. Li [15, 28, 29] proposes for biomedical applications alloys from the Ti-Mo-Si system processed by powder metallurgy due to an excellent combination of high mechanical strength, low elasticity module, a wide range of deformations, over 21.504% and a very good biocompatibility given by β-phase structure. Almeida [3] investigated the Ti-Mo alloys system processed but using laser technology, proposing for orthopedic applications an

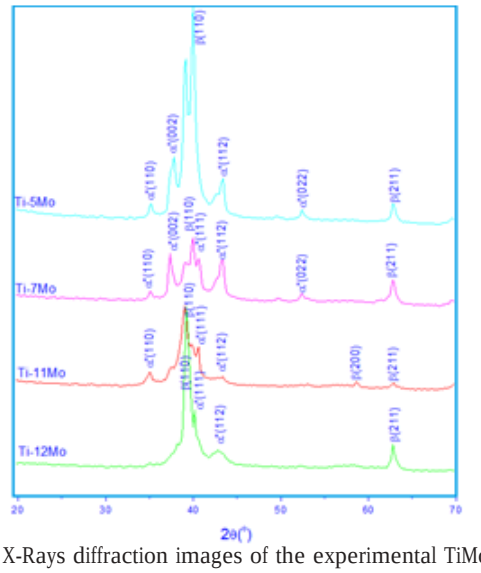

Fig. 3. X-Rays diffraction images of the experimental TiMo alloys

alloy with 13% Mo, with a modulus of 75GPa and a hardness of 240 VHN.

The results of the structural analysis performed at scanning electron microscope, for the Ti-Mo alloys are shown summarized in figure 4. The results obtained by scanning electron microscope analysis are consistent with observations from metallographic optical microscope and X-ray diffraction analysis, certifying chemical composition resulting from the initial design and analytical spectrometry analysis.

The results of metallographic aspects of experimental alloys after heat treatment for annealing solution are shown in figure 5. The analysis reveals that after water cooling martensitic type structures may be obtained and the smoothness of the martensite increases with the Mo content. Thus, the smoothness martensite is achieved at TiMo12. In the treatment of annealing solution with an air cooling the structures are highly similar, with obtaining a coarse acicular martensite.

The results of the wear behavior of experimental Ti-Mo alloys are shown in figure 6 ÷ 9 (concerning the profilometry and morphology aspects of the track wear). Test conditions used a simulated aging process may possibly between metal implant and cement. The phenomenon of wear is quite aggressive, as confirmed by the high value of the volume of wear, and also the wear rate calculated after the test. The measured and extrapolated value analysis allows the following observations (synthetic shown in fig. 10a):

- at the TiMo5 alloy wear volume values are highest being located in a very wide range respectively 0.792 ÷ 2.79 mm^3, the highest value 2.79mm^3 corresponding to the alloy in heat treated state at 950°C/1h/water and the lowest value 0.792mm^3 for the cast alloy;
- the TiMo7 and TiMo11 alloys, have similar behavior, with values of wear volume located within a reduced range, respectively of 0.6 ÷ 0.645 for TiMo7 alloy and 0.542 ÷ 0.643 for TiMo11 alloy;
- at the TiMo12 alloy the lowest values of wear volume for all states of heat treatment are obtained, respectively between 0.348 ÷ 0.64 mm^3.

Regarding the wear rate (fig. 10b), the alloys follows the same behavior observations:

- the $TiMo_5$ alloy has the highest wear rate values ranging $3.16.10^{-4}mm^2$ / Nm for cast alloy, a $10.34.10^{-4}mm^2$/

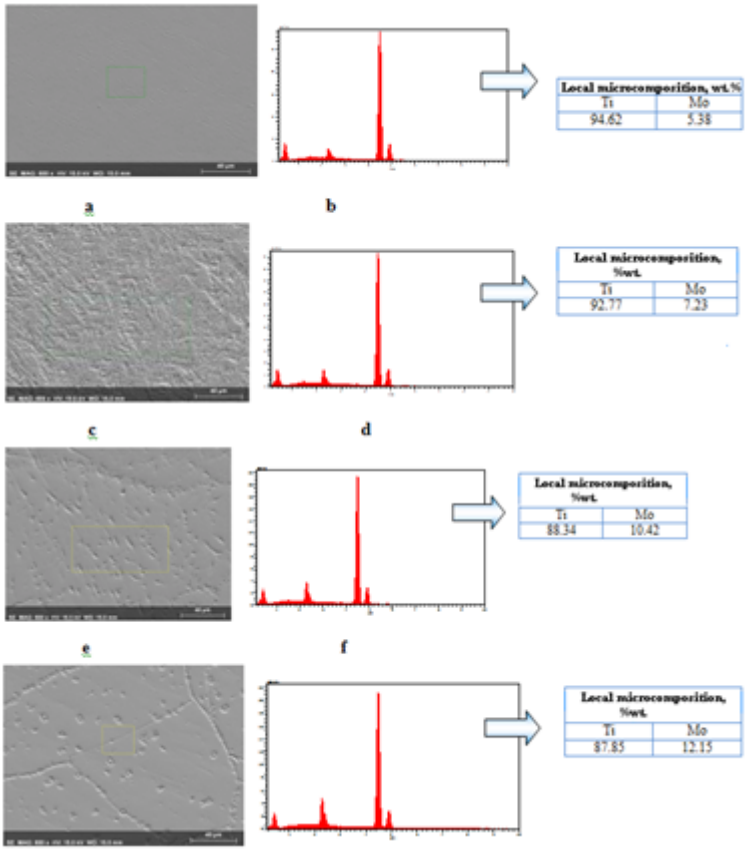

Fig.4. SEM imagines (a,c,e,g) and EDAX spectrum of local microcomposition(b,d,f,h)

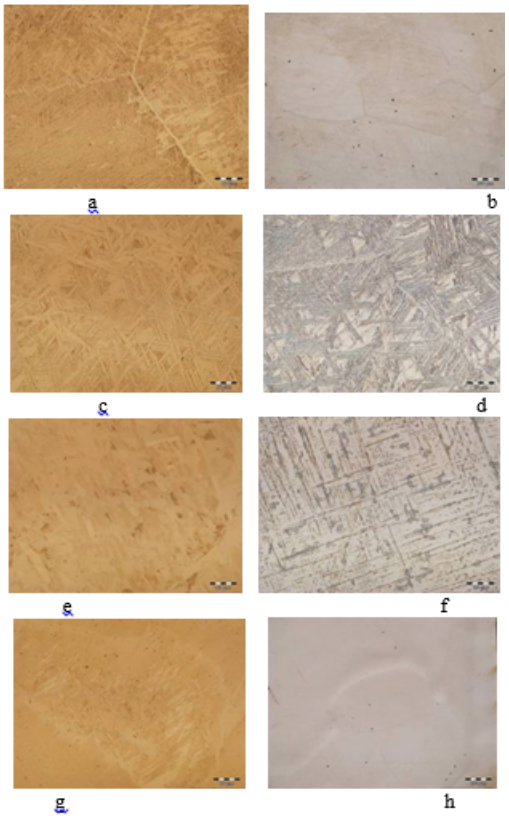

Fig.5. Microstructural aspect of TiMo alloys after heat treatments: annealing at 950°C/ 1h/water cooling (a,c,e,g); annealing at 950°C/ 1h/air cooling (b,d,f,h); $TiMo_5$ alloy (a,b); $TiMo_7$ alloy (c,d); $TiMo_{11}$ alloy (e,f); $TiMo_{12}$ alloy (g,h)

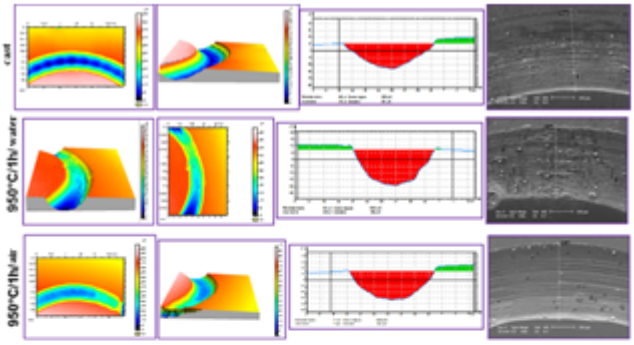

Fig. 6. Wear behaviour of the TiMo5 alloy in different states

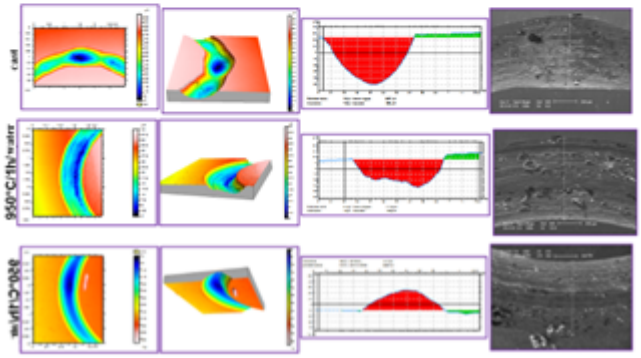

Fig. 7. Wear behaviour of the TiMo7 alloy in different states

Nm for alloy heat treated at 950°C/1h/water reaching to $5.03.10^{-4}mm^2/Nm$ for the alloy heat treated at 950°C/1h/air;

- te $TiMo_7$ and $TiMO_{11}$ alloys are relatively near to the rate of wear, respectively $2.4 \div 2.52x10^{-4}mm^2/Nm$ for TiMo7 and $2.16 \div 2.57.10^{-4}mm^2/Nm$ for TiMo11;

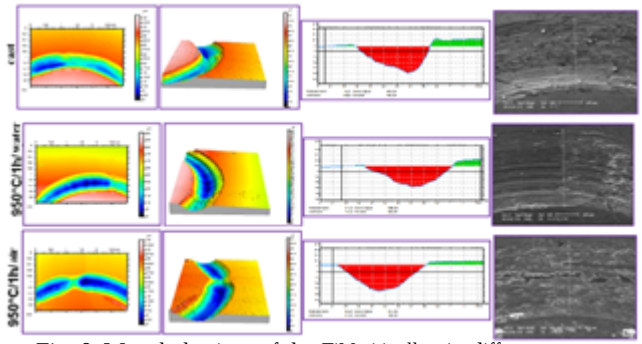

Fig. 8. Wear behaviour of the TiMo11 alloy in different states

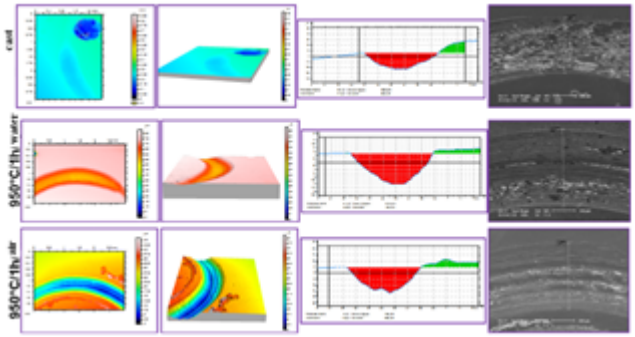

Fig. 9. Wear behaviour of the TiMo12 alloy in different states

Table 2

MORPHOLOGY OBSERVATIONS OF THE WEAR TRACK FOR THE EXPERIMENTAL TiMo ALLOYS MADE ON SCANNING ELECTRON MICROSCOPE

Alloy	State	Remarks
$TiMo_5$	cast	Scratches, parallel phonographic grip and Al_2O_3 particles deposited on the material, semi-elliptical profile of footprint
	950°C /1h/water	Very fine scratches, grip and nonuniform fine and grobe Al_2O_3 particles deposited on the material, semi-elliptical profile of footprint
	950°C /1h/air	Very fine scratches, grip on the entire surface of about 50µm, semi-sphere profile of footprint
$TiMo_7$	cast	Numerous particles of Al_2O_3 deposits on the material surface, semi-sphere profile of footprint
	950°C /1h/water	Scratches, numerouse Rizuri, numeroase grip and voids on materials and very fine particles of Al_2O_3 deposited on the materials surface, nonuniform profile of the footprint
	950°C /1h/air	Wide treads, numerous uprooting materials and Al_2O_3 particles deposited on the materials, semi-elliptical profile of footprint
$TiMo_{11}$	cast	Relative deep scratches, materials grip and fine particle of Al_2O_3 deposited on material surface, nonuniform profile
	950°C /1h/water	Scratches, grip and cracks, semi-elliptical profile of footprint
	950°C /1h/air	Very fine scratches, material grips on big fields over 400µm and particles of Al_2O_3 deposited on ring, almost semi-sphere profile of footprint

$TiMo_{12}$	cast	No scratches, the presence of dimples may indicate and possible disolution and grip of materials and particles of Al_2O_3 deposited on materials surface, semi-elliptical profile of footprint
	950°C /1h/water	Fine scratches, numerous grip with diameters over 10-100μm şi agglommeration of particle Al_2O_3 deposited on the surface material, semi-elliptical profile of footprint
	950°C /1h/air	Very fine scratches, small and big particles of Al_2O_3 deposited on the materials surface, nonuniform profile of the footprint

- the lowest values of wear rate can by observed at TiMo12 alloy heat treatment for all states and having in a very narrow field, respectively 1.39 ÷ 1.45x10^{-4}mm^2/Nm.

The observations regarding to the morphology of experimental alloys wear tracks are shown in table 2, in which notes the following conclusions:

- the TiMo5 and TiMo7 alloys have in the traces of wear many scratches parallel phonographic deep profiles of all sign of abrasive wear mechanism;

- tThe TiMo11 and TiMo12 alloys were less prominent phonographic which can be observe snatching material and numerous adherent Al_2O_3 particles sign of wear by adhesion mechanism.

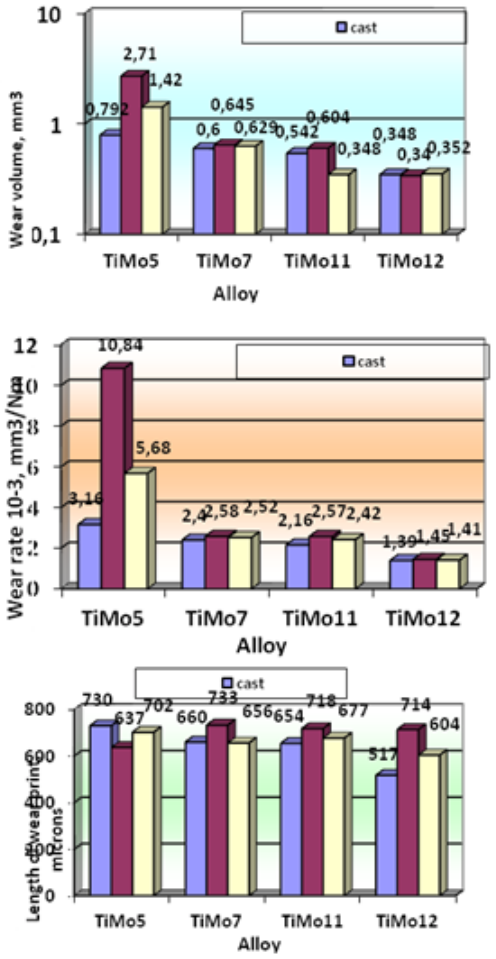

Fig. 10. Volume wear rate (a) wear rate (b) and length of wear track (c) of the TiMo experimental alloys after testing in Ringer solution at Talysurf profilometer

Regarding the wear track width as shown in figure 10c there is no correlation between the mode and amount of alloying, only the sizes between 517 ÷ 733μm.

The morphology of the footprint after wear test were put in evidence by scaning electron microscopy, as is given in table 2. Regarding the wear track width, there is no correlation between manner of alloying and wear length, observing tracks about 517 ÷ 733μm.

Conclusions

In the present paper there are given the results concerning the structure and wear behaviour of four TiMo alloys, respectively TiMo5, TiMo7, TiMo11 and TiMo12. Phasic constitution of the TiMo experimental alloys showed that alloys TiMo5 and TiMo7 have a dual phase structure, consisting of a high proportion of orthorhombic martensite α'' and small proportion of β solid solution. On increasing the concentration of molybdenum content, respectively alloys TiMo11 and TiMo12, the quantitative proportion of b solid solution increases without complete elimination of orthogonal martensite.

Wear behaviour of some new titanium-molybdenum alloys was performed on a profilometer by measuring and then extrapolating the values concerning amount of wear. Finally the wear rates were determined for the new TiMo alloys. It was such a simulated wear process may possibly between implant and cement. The wear volume values of TiMo5alloy are the highest, being located in a very broad, about 0.792 ÷ 2.79 mm^3, the highest value corresponding to the heat treated alloy at 950° C /1h/water (2.79mm^3) and the lowest value for the cast alloy (respectively 0.792 mm^3). Alloys TiMo7 and TiMo11 have similar behavior, with wear volume values located within 0.6 ÷ 0.645 mm^3 for TiMo7 alloy and 0.542÷0.643 for TiMo11 At the TiMo12 alloy the lowest values of wear volume for all states of heat treatment were obtained, in the range 0.348 ÷ 0.64 mm^3. In terms of wear rate, TiMo5 alloy has the highest wear rate values ranging from 3.16.10^{-4}mm^2 / Nm for cast state, about 10.34.10^{-4}mm^2 / Nm for 950°C /1h/water state, reaching to 5.03.10^{-4}mm^2 / Nm for the alloy heat treated at 950°C/1h/air. The TiMo7 and TiMO11 alloys are relatively close to the rate of wear, namely 2.4÷2.52.10^{-4} mm^2/Nm for TiMo7 and 2.16 ÷ 2.57 mm^2/Nm for TiMo11. The lowest values of wear rate stands at TiMo12 alloy for all states and located in a very narrow field, about 1.39 ÷ 1.45.10^{-4} mm^2/Nm. It can highlight the beneficial influence of molybdenum alloying with regarding the wear behavior of the alloy TiMo12 having the lowest values of wear rate. Observations of the morphology of wear tracks showed that TiMo5 alloys and traces of wear TiMo7 have many scratches parallel phonographic deep profiles of all, a sign of abrasive wear mechanism. Alloys TiMo12 TiMo11 have scratches less prominent, which stands snatching material and numerous adherent Al_2O_3 particles, a sign of the adhesive wear mechanism. Regarding the wear track width, there is no correlation between manner of alloying and wear length, observing tracks about 517 ÷ 733μm.

Acknowledgements: This work was supported by Romanian POSDRU projects number 60203 and /159/1.5S/132397, entitled Excellence in research by doctoral and postdoctoral scholarships. All the authors have the same contribution to the paper, which is a multidisciplinary research.

References

1. ATAPOUR, M., et al., Corrosion behavior of â titanium alloys for biomedical applications. Materials Science and Engineering: C, 2011. 31(5): p. 885-891.

2. BACHE, M.R., A review of dwell sensitive fatigue in titanium alloys: the role of microstructure, texture and operating conditions. International Journal of Fatigue, 2003. 25(9-11): p. 1079-1087.
3. *** Materials Science and Engineering: C, 2012. 32(5): p. 1190-1195.
4. NIINOMI, M., Fatigue characteristics of metallic biomaterials. International Journal of Fatigue, 2007. 29(6): p. 992-1000.
5. GERINGER, J., B. FOREST, AND P. Combrade, Fretting-corrosion of materials used as orthopaedic implants. Wear, 2005. 259(7–12): p. 943-951.
6. GEETHA, M., et al., Ti based biomaterials, the ultimate choice for orthopaedic implants – A review. Progress in Materials Science, 2009. 54(3): p. 397-425.
7. MORE, N.S., et al., Tribocorrosion behavior of βtitanium alloys in physiological solutions containing synovial components. Materials Science and Engineering: C, 2011. 31(2): p. 400-408.
8. NIINOMI, M., Fatigue performance and cyto-toxicity of low rigidity titanium alloy, Ti–29Nb–13Ta–4.6Zr. Biomaterials, 2003. 24(16): p. 2673-2683.
9. GONZALEZ, J.E.G. AND J.C. MIRZA-ROSCA, Study of the corrosion behavior of titanium and some of its alloys for biomedical and dental implant applications. Journal of Electroanalytical Chemistry, 1999. 471(2): p. 109-115.
10.AL-MAYOUF, A.M., et al., Corrosion behavior of a new titanium alloy for dental implant applications in fluoride media. Materials Chemistry and Physics, 2004. 86(2–3): p. 320-329.
11.ANTUNES, R.A. AND M.C.L. DE OLIVEIRA, Corrosion fatigue of biomedical metallic alloys: Mechanisms and mitigation. Acta Biomaterialia, 2012. 8(3): p. 937-962.
12.BUCHANAN RA, R.E.J., WILLIAMS JM, Wear-accelerated corrosion of Ti6Al4V and nitrogen-ion-implanted Ti6Al4V: mechanism and influence of fixed-stress magnitude. Journal Biomed Mater Res, 1987. 21: p. 367-377.
13.DAVIS, J.R., Overview of Biomaterials and Their Use in Medical Devices. 2003: ASM International.
14.KHAN, M.A., R.L. WILLIAMS, AND D.F. WILLIAMS, In-vitro corrosion and wear of titanium alloys in the biological environment. Biomaterials, 1996. 17(22): p. 2117-2126.
15.LI, C., Y. ZHAN, AND W. JIANG, â-Type Ti–Mo–Si ternary alloys designed for biomedical applications. Materials & Design, 2012. 34(0): p. 479-482.
16. HO, W.F., C.P. JU, AND J.H. CHERN LIN, Structure and properties of cast binary Ti–Mo alloys. Biomaterials, 1999. 20(22): p. 2115-2122.
17. Ho, W.-F., et al., Structure and mechanical properties of Ti–5Cr based alloy with Mo addition. Materials Science and Engineering: C, 2010. 30(6): p. 904-909.
18. LIN, D.J., J.H. CHERN LIN, AND C.P. JU, Effect of omega phase on deformation behavior of Ti–7.5Mo–xFe alloys. Materials Chemistry and Physics, 2002. 76(2): p. 191-197.
19. LIN, D.J., J.H. CHERN LIN, AND C.P. JU, Structure and properties of Ti–7.5Mo–xFe alloys. Biomaterials, 2002. 23(8): p. 1723-1730.
20. LIN, D.-J., et al., Bone formation at the surface of low modulus Ti–7.5Mo implants in rabbit femur. Biomaterials, 2007. 28(16): p. 2582-2589.
21. CHEN YU-YONG, X.L.-J., LIU ZHI-GUANG,KONG FAN-TAO,CHEN ZI-YONG, Microstructures and properties of titanium alloys Ti-Mo for dental use. Science Press China, 2006. 16: p. 824-828.
22. OLIVEIRA, N.T.C., et al., Development of Ti–Mo alloys for biomedical applications: Microstructure and electrochemical characterization. Materials Science and Engineering: A, 2007. 452–453(0): p. 727-731.
23. WU, E., et al., Formation of a tetragonal phase hydride in Ti–Mo–H system. Journal of Alloys and Compounds, 2008. 458(1–2): p. 161-165.
24. GORDIN, D.M., et al., Synthesis, structure and electrochemical behavior of a beta Ti-12Mo-5Ta alloy as new biomaterial. Materials Letters, 2005. 59(23): p. 2936-2941.
25. GORDIN, D.M., ET AL., Microstructural characterization of nitrided beta Ti–Mo alloys at 1400°C. Materials Characterization, 2010. 61(3): p. 376-380.
26. GABRIEL, S.B., ET AL., Characterization of a new beta titanium alloy, Ti–12Mo–3Nb, for biomedical applications. Journal of Alloys and Compounds, 2012. 536, Supplement 1(0): p. S208-S210.
27. ZHOU, Y.-L. AND D.-M. LUO, Microstructures and mechanical properties of Ti–Mo alloys cold-rolled and heat treated. Materials Characterization, 2011. 62(10): p. 931-937.
28. LI, L., I. ETSION, AND F.E. TALKE, The effect of frequency on fretting in a micro-spherical contact. Wear, 2011. 270(11–12): p. 857-865.
29. LI, S.J., et al., Fatigue properties of a metastable â-type titanium alloy with reversible phase transformation. Acta Biomaterialia, 2008. 4(2): p. 305-317.
30. ROSU, S., FLAVIUS, P., TATU RF., Abs 3d Printed Facial Study Model Using Hermite Matrix Interpolation For Manufacturing Facial Epistasis, Mat.Plast, **51**, no.3, 2014, p.290
31. CAPLESCU, CR., MARSAVINA, L., BORDEASU, I., SEKEI, R., Mat.Plast., **47**, no.3, 2009, p.379

Manuscript received: 29.09.2015